PERGAMON International Journal of Multiphase Flow 24 (1998) 1183–1203

International Journal of Multiphase Flow

Pressure gradient in horizontal liquid–liquid flows

P. Angeli *, G.F. Hewitt

Department of Chemical Engineering and Chemical Technology, Imperial College of Science, Technology and Medicine, Prince Consort Road, London SW7 2BY, UK

Received 22 July 1997; received in revised form 25 January 1998

Abstract

Pressure gradients were measured during the cocurrent flow of a low viscosity oil (1.6 mPa s viscosity and 801 kg/m^3 density) and water in two 1-inch nominal bore horizontal test sections made from stainless steel and acrylic resin, respectively. Measurements were made for mixture velocities from 0.3 to 3.9 m/s and for water volume fractions from 0 to 100%. The main finding is the large difference between the results for the respective tube materials which cannot be explained only in terms of the difference in tube roughness. It is postulated that the different wettability characteristics of the two pipe materials are also responsible for this disparity. Furthermore, it was found that at high mixture velocities, where dispersed flow patterns prevail, there is a peak in pressure gradient during phase inversion and an apparent drag reduction effect when oil is the continuous phase.

Keywords: Liquid–liquid flow; Pressure gradient; Stratified flow; Dispersed flow; Phase inversion; Wettability

1. Introduction

Liquid–liquid flows have many applications in a diverse range of process industries and particularly in the petroleum industry, where oil and water are often produced and transported together. However, despite their importance, such flows have not been explored to the same extent of the gas–liquid flows. As a result the most common predictive theories for pressure gradient that are used in liquid–liquid flows are developments of models created for gas–liquid flows. Although the main application of such flows has been in the transport of oil–water mixtures in steel pipelines, most of the (rather limited) experimental work has been carried out

* Corresponding author. Present address: Department of Chemical Engineering, University College London, Torrington Place, London WC1E 7JE, UK.

PII: S0301-9322(98)00006-8

in glass or acrylic pipes. These have, of course, the advantage of being transparent, allowing the flow to be viewed; however, their wall properties (roughness and wettability) may be very different to those of steel tubes and this may affect the design parameters such as the pressure drop. The work described here was focused on evaluating the effect of tube surface on pressure gradient; as will be seen these effects can be very considerable (typically up to 100% difference in pressure gradient between the steel and the acrylic resin tubes).

In order to investigate the pipe flow behaviour of liquid–liquid two phase systems, an experimental flow facility has been constructed at Imperial College. Pressure gradients were measured for a wide range of flowrates in two horizontal test sections that have different wall properties. In what follows, Section 2 gives a brief summary of the existing literature on the subject, Section 3 describes the experimental system, Section 4 gives the results obtained during the horizontal liquid–liquid flow in both test pipes and finally Section 5 summarizes the conclusions.

2. Literature review

Interest in oil–water flows arose in the 1950's from the realization that addition of water to crude oil could reduce the pressure gradient (Russell and Charles, 1959; Russell et al., 1959; Charles et al., 1961). After a relatively quiescent period, interest in the field is now growing again because of the simultaneous production of oil and water from many currently operating fields.

The approaches adopted for the correlation and prediction of oil–water flows fall into the following categories:

(1) Methods which are purely empirical in nature.

(2) Methods which take into consideration the fact that the flow is occurring in a specific flow pattern (stratified or dispersed for instance).

These approaches are discussed further below. However, to the knowledge of the present authors, the influence of the pipe wall characteristics has not been systematically investigated before this study.

2.1. Empirical correlations

Charles and Lilleleht (1966) used the empirical parameters X and Φ, suggested by Lockhart and Martinelli (1949) for gas–liquid pipeline flow, to represent pressure gradient data of stratified liquid–liquid flows. In this case the parameters X and Φ were defined as follows:

$$X^2 = \frac{(\mathrm{d}p/\mathrm{d}z)_\mathrm{o}}{(\mathrm{d}p/\mathrm{d}z)_\mathrm{w}} \tag{1}$$

where $(\mathrm{d}p/\mathrm{d}z)_\mathrm{o}$ and $(\mathrm{d}p/\mathrm{d}z)_\mathrm{w}$ are the pressure gradients for the oil and water phases flowing alone in the channel, respectively, and

$$\Phi^2 = \frac{(\mathrm{d}p/\mathrm{d}z)_\mathrm{TP}}{(\mathrm{d}p/\mathrm{d}z)_\mathrm{o}} \tag{2}$$

where $(dp/dz)_{TP}$ is the two-phase (oil–water mixture) pressure gradient. When Charles and Lilleleht used the above parameters to represent their experimental data, the resulting curve was shifted from the Lockhart–Martinelli one for gas–liquid flow. Theissing (1980) attributed this difference in the two curves to the density ratio difference that exists between a gas–liquid and a liquid–liquid system. His multi-parameter correlation for two-phase flow pressure gradient, which can be used both for gas–liquid and liquid–liquid flows, is described by the following equations:

$$(dp/dz)_{TP} = \left[(dp/dz)_{otM}^{1/ne} \left(\frac{\dot{M}_o}{\dot{M}_t} \right)^{1/e} + (dp/dz)_{wtM}^{1/ne} \left(\frac{\dot{M}_w}{\dot{M}_t} \right)^{1/e} \right]^{ne} \tag{3}$$

where,

$$e = 3 - 2\left(\frac{2\sqrt{\rho_o/\rho_w}}{1+\rho_o/\rho_w} \right)^{0.7/n} \tag{4}$$

$$n = \frac{n_1 + (1/X)^{0.2} n_2}{1 + (1/X)^{0.2}} \tag{5}$$

$$n_1 = \frac{\ln\left((dp/dz)_{oM}/(dp/dz)_{otM}\right)}{\ln\left(\dot{M}_o/\dot{M}_t\right)} \qquad n_2 = \frac{\ln\left((dp/dz)_{wM}/(dp/dz)_{wtM}\right)}{\ln\left(\dot{M}_w/\dot{M}_t\right)} \tag{6}$$

where ρ_o, ρ_w are the densities of the oil and the water, respectively, $\dot{M}_o$ and $\dot{M}_w$ are the mass flow rates of the oil and the water, respectively, $(dp/dz)_{oM}$ and $(dp/dz)_{wM}$ are the pressure gradients when the oil or the water flows alone at $\dot{M}_o$ or $\dot{M}_w$, respectively, and $(dp/dz)_{otM}$ and $(dp/dz)_{wtM}$ are the pressure gradients if the oil or the water flowed alone at the total mixture mass rate of flow $(\dot{M}_o + \dot{M}_w)$.

Stapelberg and Mewes (1994) also used the parameters X and Φ to represent their experimental pressure gradients taken in two pipes with different diameters. Although the data followed a similar trend to that of Charles and Lilleleht (1966), there was an obvious effect of the pipe diameter. Their results also showed that a single model is not sufficient to correlate the pressure gradient data in all the regimes of liquid–liquid flow.

2.2. Methods based on flow patterns

2.2.1. Stratified flow

Basically there have been two main approaches to modelling stratified flow. The first approach involves the analytical solution of the Navier–Stokes equations for the full flow field taking account of the interface. Examples of the analytical approach are the studies of Kurban (1997) for a planar interface, while Moalem Maron et al. (1995) took into account the curvature of the interface. This approach though is restricted to laminar flows and cannot be applied to the turbulent flows encountered in the present work. There have also been attempts

to solve the problem numerically (Charles and Redberger, 1962; Hall and Hewitt, 1993; Kurban, 1997).

The second approach follows the theoretical analysis of Taitel and Dukler (1976a) for gas–liquid flows (Taitel and Dukler, 1976b; Brauner and Moalem Maron, 1989; Kurban et al., 1995). Oil and water are represented as two separate regions and empirical correlations are used for the wall and the interfacial shear stresses (the 'two-fluid' model). Considering smooth stratified flow in equilibrium, where the pipe is horizontal, the momentum balance for the respective phases is:

$$\text{water phase: } -A_w\left(\frac{dp}{dz}\right) - \tau_{W_w}P_w - \tau_i P_i = 0 \tag{7}$$

$$\text{oil phase: } -A_o\left(\frac{dp}{dz}\right) - \tau_{W_o}P_o + \tau_i P_i = 0 \tag{8}$$

where, A_o and A_w are the cross sectional areas of the oil and the water phase, respectively, (dp/dz) is the two-phase pressure gradient, τ_{W_o} and τ_{W_w} are the wall shear stresses for the oil and the water, respectively, τ_i is the interfacial oil–water shear stress, P_o and P_w are the oil-wetted and water-wetted wall peripheries, respectively, and P_i is the interfacial periphery where τ_i acts on. The shear stresses are calculated by invoking empirical friction factor relationships for the wall and the interface. If the interfacial shear stress is set equal to the water wall shear stress, and non-dimensional parameters are used, then from Eqs. (7) and (8) the following can be derived:

$$X^2\left(\frac{\tilde{D}_{H_o}\tilde{u}_o}{\tilde{D}_{H_w}\tilde{u}_w}\right)^{-m}\left(\frac{\tilde{u}_o}{\tilde{u}_w}\right)^2\frac{\tilde{P}_o}{\tilde{A}_o} - \frac{\tilde{P}_w}{\tilde{A}_w} - \tilde{P}_i\left(\frac{1}{\tilde{A}_o}+\frac{1}{\tilde{A}_w}\right) = 0 \tag{9}$$

$$\Phi^2 = \frac{1}{4\tilde{A}_w X^2}\left(\tilde{D}_{H_w}\tilde{u}_w\right)^{-m}\tilde{u}_w^2\left(\tilde{P}_o+\tilde{P}_w\right) \tag{10}$$

where the tilde ($\sim$) denotes the dimensionless quantities, $\tilde{u}_o$ and $\tilde{u}_w$ are the dimensionless velocities of the oil and the water phase, respectively, m is the Reynolds number exponent in the calculation of the friction factors, and $\tilde{D}_{H_o}$ and $\tilde{D}_{H_w}$ are the dimensionless hydraulic diameters for the oil and the water flow, respectively. Since in Eqs. (9) and (10) all the dimensionless parameters depend on the height of the interface, h_w, from Eq. (9) h_w can be calculated. Then Eq. (10) will give Φ (defined in Eq. (2)), which can be used for the estimation of the two-phase pressure gradient.

2.2.2. Dispersed flow

For dispersed liquid–liquid flows the homogeneous model is obviously a candidate route for the prediction of the pressure gradient. In this model the mixture of the two fluids is treated as a 'pseudofluid' with suitably averaged properties, that obeys the usual equations of single phase flow. The main problem in applying this approach is in the calculation of the effective mixture

viscosity, particularly since the viscosity can have anomalous behaviour during liquid–liquid flow. The calculation of the viscosity in liquid–liquid dispersions is discussed in Section 2.2.3.

2.2.3. Viscosity of liquid–liquid dispersions

A number of relationships have been proposed for averaging the viscosities of the phases in dispersed flows. Dukler et al. (1964) for gas–liquid flows proposed averaging in terms of flow volume fractions of the phases. By applying the same principle in oil–water flows the mixture viscosity η_m becomes:

$$\eta_m = \varepsilon_o \eta_o + \varepsilon_w \eta_w \tag{11}$$

where ε_o and ε_w are the oil and water flow volume fractions, respectively, and η_o and η_w are the oil and water viscosities, respectively.

Brinkman (1952) and Roscoe (1952) both starting from Einstein's relationship for viscosity of suspensions in extreme dilution, proved mathematically that the viscosity η_m of a suspension of non-uniform spheres can be given by:

$$\eta_m = \eta_c (1 - \varphi)^{-2.5} \tag{12}$$

where η_c is the continuous phase viscosity and φ is the volume fraction of the dispersed phase.

Several investigators have studied the flow behaviour of oil–water dispersions in pipe viscometers, where the two fluids were premixed and the pressure gradient of the mixture was measured during its flow in a pipe. Earlier work concentrated on the oil-in-water dispersions. Cengel et al. (1962) worked with different volume fractions of the dispersed oil phase in laminar and turbulent flows in horizontal and vertical pipes. The authors argued that the dispersions behaved like Newtonian fluids, apart from the case of dense dispersions in horizontal flow where the measured friction factor f was not proportional to $Re_c^{-0.25}$ (where Re_c is the continuous phase Reynolds number). Their results also showed that the apparent viscosities of the dispersions in vertical turbulent flow (calculated from the Blasius formula) seemed to be lower than those in laminar flow (calculated from a corrected form of the Hagen–Poiseuille formula). Newtonian behaviour of oil-in-water dispersions in vertical turbulent flow was also observed by Faruqui and Knudsen (1962) and Ward and Knudsen (1967).

Pal (1993) presented data on oil-in-water dispersions in laminar and turbulent horizontal flow. He showed that the apparent viscosities of the dispersions in laminar flow were higher than those in the turbulent flow implying that there is a *drag reduction* in turbulent flow. He also worked with water-in-oil dispersions where the drag reduction was more prominent than in oil-in-water dispersions. Charles et al. (1961) had also observed a reduction in pressure gradient resulting from the addition of water to oil, when the resultant regime was water drops in oil. Martinez et al. (1988) experimenting with oil-in-water dispersions in laminar flow found Newtonian behaviour when the dispersed phase volume fraction was up to 10% and pseudoplastic behaviour above it.

Equations of the type proposed by Brinkman (Eq. (12) imply a peak in viscosity at the phase inversion point. *Phase inversion* of a dispersion of two immiscible liquids is defined as the transition of a phase from being dispersed to being continuous and vice versa. The *phase*

inversion point is defined as the volume fraction of the dispersed phase above which this phase will become continuous. For two immiscible liquids there is a range of volume fractions over which either component can be the dispersed phase. This range, where phase inversion may occur, is called the *ambivalent range*. Within the ambivalent range a variety of factors will determine the exact phase inversion point, like the viscosities of the two fluids, their density difference and the temperature (Selker and Sleicher, 1965; Luhning and Sawistowski, 1971; McClarey and Mansoori, 1978; Arirachakaran et al., 1989). The way in which the dispersion is initialised (Selker and Sleicher, 1965; Efthimiadu et al., 1994), as well as the wetting properties of the construction material of the mixture container (Guilinger et al., 1988) can also affect phase inversion. However, most of the available information in the literature regarding the importance of the above factors comes from experiments in stirred tanks.

It has been observed that the viscosity of a dispersion increases at the phase inversion point (Guilinger et al., 1988; Pal, 1993). From experiments in pipeline flow of oil and water, Guzhov et al. (1973) and Arirachakaran et al. (1989) observed a peak in the measured frictional pressure drop during dispersed flow which they attributed to the phase inversion. In similar experiments Nädler and Mewes (1995) found two peaks in the pressure gradient; they related the first to a transition from water-in-oil dispersed flow to stratified/dispersed flow and the second to a transition from stratified/dispersed flow to an oil-in-water dispersed flow.

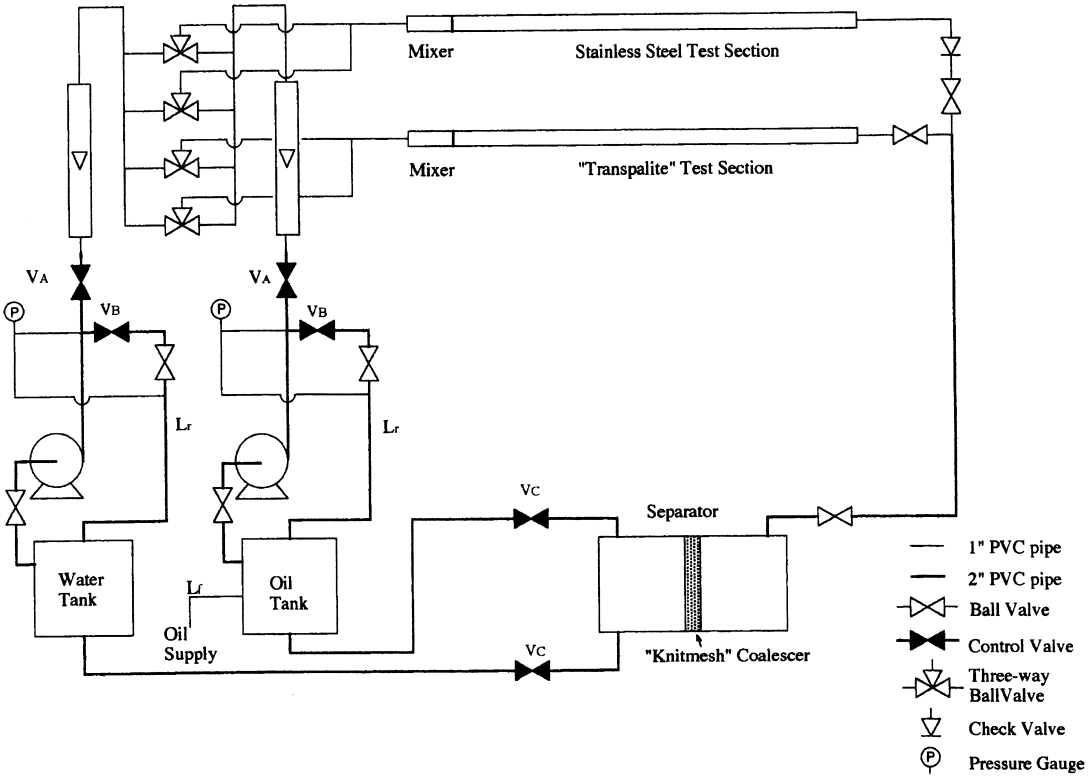

Fig. 1. Liquid–liquid flow facility at Imperial College.

The objective of the present work was to obtain more experimental data for oil-water flows, especially in the dispersed region with particular reference to the effect of the tube material. The data was aimed at supplementing and extending the limited range of information available in the literature.

3. Experimental system

Pressure gradient data during the horizontal flow of oil and water were obtained using the flow facility shown schematically in Fig. 1, which is described in detail by Angeli (1996). Water and oil were metered and supplied separately from two storage tanks to either one of two test sections, made from stainless steel and Transpalite™ (a type of acrylic resin), respectively. The steel pipe has 24.3 mm ID and 9.7 m total length and the acrylic pipe has 24 mm ID and 9.5 m total length. The test sections were made up from several flanged lengths of the respective tubes and care was taken to ensure that the bore was continuous (i.e. without steps at the flange positions). The water was introduced at the end of the tube and the oil through a T-junction at the bottom of the tube about 15 cm downstream of the end of the tube. The mixture of the two fluids, passed from this test section to a horizontal 1.94 m long, 0.54 m ID, liquid–liquid separation vessel, equipped internally with a Knitmesh coalescer. A short transparent acrylic pipe, 10 cm long, that could be placed between any two flanges, was used for visualization of the flow in the steel test section.

The flowrates of the fluids were measured with variable area flowmeters, calibrated for the appropriate fluid with an accuracy of $\pm 1\%$ of the maximum flowrate. Pressure drop was measured with a Validyne DP45 variable reluctance differential pressure transducer with interchangeable diaphragm. The transducer has a $\pm 0.25\%$ full scale accuracy. The pressure drop was measured over a distance of 1.9 m in the stainless steel test section (starting at about 5 m from the inlet) and over a distance of 2.5 m in the acrylic test section (starting at about 4 m from the inlet). The liquids that were used in the experiments reported in this paper were tap water and kerosene (EXXSOL D80), with properties shown in Table 1. Tap water was used for convenience and also made subsequent measurements involving the conductivity of the phases (Angeli, 1996) easier, since the use of distilled/deionised water would involve the addition of some salt. The tap water used had a surface tension (66 dyn/cm) close to that of pure water (70 dyn/cm) indicating that surface active components were minimal.

Pressure gradients were measured in both pipes for mixture velocities ranging from 0.3 to 3.9 m/s and input water volume fractions ranging from 0 to 100%. The full set of experimental

Table 1
Oil properties at 20°C

Product name	EXXSOL D80
Density	801 kg/m^3
Viscosity	1.6 mPa s
Interfacial tension air–oil	0.027 N/m
Interfacial tension oil–water	0.017 N/m

Table 2
Experimental pressure gradient data: Steel pipe

Pressure gradient (Pa/m)													
Water superficial velocity (m/s)	Oil superficial velocity (m/s)												
	0.11	0.22	0.32	0.43	0.54	0.65	0.86	1.08	1.29	1.51	1.72	2.16	2.59
0.11	79.06	115.11	156.99	212.80	307.47	328.96	521.58	736.04	990.73	1276.19	1554.75		
0.22	154.56	212.85	252.24	304.43	342.58	417.29	606.71	799.27	1081.97	1408.01	1661.05		
0.32	220.57	293.32	381.93	460.10	502.06	581.36	736.66	908.68	1165.58	1500.98	1811.43		
0.43	315.91	436.27	586.92	680.18	700.86		847.67		1241.79		1987.98	2551.84	3552.07
0.54	416.57	590.78	786.74	920.27	1050.03								
0.86				1007.39			1703.78		2760.04		2592.73	3224.29	4102.82
1.29				1528.69			2363.27		3549.88		4932.92	6525.83	5451.76
1.72				2437.32			3452.15		4824.21		6363.56		
2.16				3588.00			4856.75		6439.14		6530.55		
2.59				4985.59			6224.07						

Table 3
Experimental pressure gradient data: Acrylic pipe

Pressure gradient (Pa/m)													
Water superficial velocity (m/s)	Oil superficial velocity (m/s)												
	0.11	0.22	0.33	0.44	0.55	0.66	0.88	1.1	1.33	1.55	1.77	2.21	2.65
0.11	33.52	72.30	118.54	164.16	238.70	301.23	428.78	576.73	833.20	1118.21	1420.62		
0.22	83.06	124.67	171.57	228.24	286.62	362.98	519.82	672.85	855.48	1086.61	1466.41		
0.33	154.47	183.02	243.80	288.39	391.27	439.76	577.13	788.86	977.92	1169.19			
0.44	209.90	262.87	323.62	385.13	425.85	500.22	633.50		992.85		1334.40	2053.45	2651.55
0.55	280.84	335.20	394.70	452.88	548.88	622.56							
0.88				798.87			1188.69		1691.14		2092.33	2517.70	3046.97
1.33				1350.59			1862.58		2495.96		3284.80	4472.43	4079.99
1.77				2004.04			2553.30		3475.43		4483.03		
2.21				2784.18			3628.22		4582.51				
2.65				3891.32			4837.09						

data is presented in Tables 2 and 3. At these flow conditions the following flow patterns were observed:

Separated flow patterns: Here the two fluids form continuous layers on the top and the bottom of the pipe according to their densities. Completely separated or *stratified flow* occurred only up to mixture velocities of around 0.3 m/s in the steel and about 0.6 m/s in the acrylic pipe. As the velocities of the phases increase the interface becomes more disturbed and drops of one liquid appear within the layer of the other. At even higher flowrates there are distinct layers of oil and water at the top and bottom of the pipe, respectively, but in the interface there exists a layer of drops (*three layer flow pattern*). This regime exists at intermediate water volume fractions (typically between 0.2 to 0.5) and at mixture velocities 0.7 to 1.3 m/s in the steel pipe and 0.9 to 1.7 m/s in the acrylic pipe.

Dispersed flow patterns: Here one fluid is continuous and the other fluid is in the form of drops dispersed in it. At the lower velocities in this regime the drops occupy only the upper or the lower layer of the pipe and leave a clear layer of the continuous phase (*stratified/mixed flow pattern*). The stratified-mixed regime appears at approximately the same mixture velocities as the three layer. At high water fractions (typically above 0.5) the continuous layer is water, while at low water fractions (typically below 0.3) the continuous layer is oil. At the higher velocities the drops are dispersed throughout the continuous phase (*dispersed flow pattern*). This regime starts at velocities of 1.3 and 1.7 m/s in the steel and the acrylic tubes, respectively.

In general and for the same mixture velocities and water fractions the flow patterns were more disturbed in the steel than in the acrylic pipe. Also oil tended to remain continuous over a larger range of conditions in the acrylic pipe (e.g. larger area of stratified/mixed with oil layer flow pattern). These differences, which are also reflected in the measured pressure gradients as will be seen below, cannot only be explained by the difference in the wall roughness between the two tubes. It is believed that the different wetting properties of the two pipe materials are also responsible for their different behaviour.

Contact angle measurements were conducted by Norsk Hydro (Valle, 1995) and showed that steel can be either oil or water wetted, depending on the history of the sample, while acrylic is preferentially wetted by oil in all cases. Furthermore, contact angles of drops of one phase in the other were measured using samples that have been previously water or oil wetted. The results are shown in Table 4.

Table 4
Contact angles on different surfaces

Material	Oil drops in water		Water drops in oil	
	water wetted	oil wetted	water wetted	oil wetted
Steel	143.3	0.0	0.0	128.7
Acrylic	87.6	84.4	106.0	121.6

4. Pressure gradient results

4.1. Single phase flow tests

The results for the single phase flow of oil and water were plotted as friction factor against Reynolds number. For each test section, the friction factors for oil and water were in close agreement. Eq. (13) by Zigrang and Sylvester (1985) (an explicit form of the Colebrook (1939)) equation was fitted to the data to estimate the roughness of each pipe:

$$\frac{1}{\sqrt{f}} = -2\log\left(\frac{\varepsilon_r/D}{3.7} - \frac{4.518}{\mathrm{Re}}\log\left(\frac{6.9}{\mathrm{Re}} + \left(\frac{\varepsilon_r/D}{3.7}\right)^{1.11}\right)\right) \tag{13}$$

where f is the wall friction factor, ε_r is the wall roughness, D is the pipe diameter, Re is the Reynolds number, $\mathrm{Re} = DU\rho/\eta$, U is the velocity of the single phase, η and ρ are the viscosity and the density of the single phase. The experimental data were fitted best for a wall roughness of 7×10^{-5} m for the steel pipe and 1×10^{-5} m for the acrylic pipe. The above values of the wall roughness will be used in the analysis below.

4.2. Comparison of the pressure gradients in the steel and the acrylic test section

In general the pressure gradients measured in the acrylic tube were lower than those measured in the steel tube. However, the differences were often much greater than what would be expected from the differences in tube roughness. To focus on the differences in behaviour, the data was non-dimensionalised by dividing the measured two-phase pressure gradient by the pressure gradient for oil flowing alone in each tube. Sample results are shown in Figs. 2–6 for total mixture velocities of 0.6, 0.8, 2.6, 3.0 and 2.1 m/s, respectively, where the non-

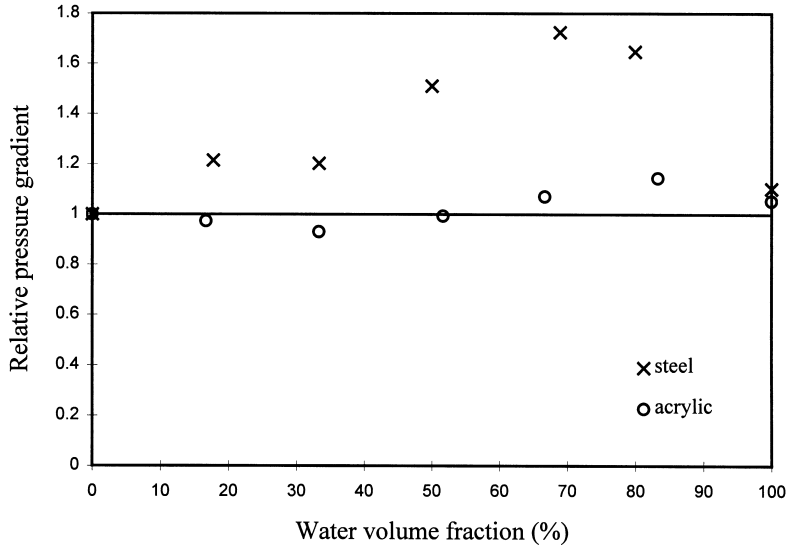

Fig. 2. Non-dimensional pressure gradients in the steel and the acrylic pipes at mixture velocity 0.6 m/s.

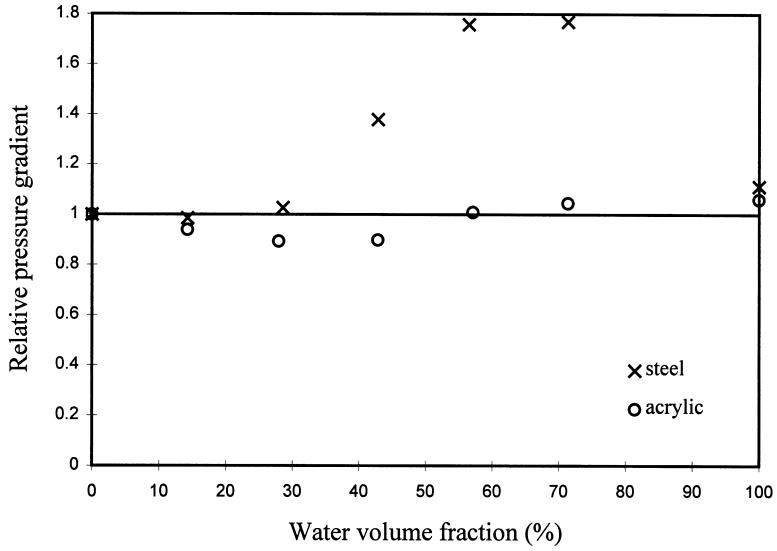

Fig. 3. Non-dimensional pressure gradients in the steel and the acrylic pipes at mixture velocity 0.8 m/s.

dimensional pressure gradient is given as a function of input water volume fraction. The following main features were revealed:

(1) At low mixture velocities (up to about 1 m/s) (Figs. 2 and 3) the pressure gradient for the acrylic tube is relatively unaffected by the water volume fraction. On the other hand the pressure gradient for the steel tube is higher especially at high water volume fractions. At these mixture velocities separated flow patterns prevail, while for the same mixture velocity the

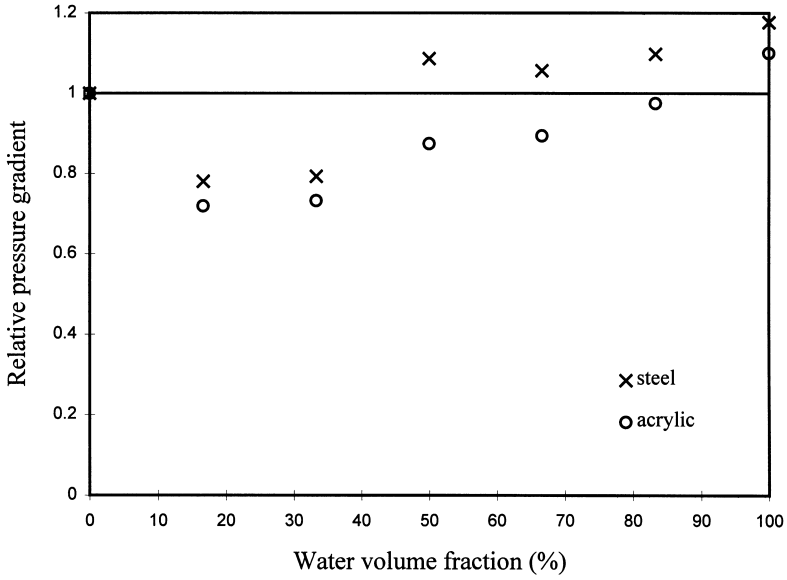

Fig. 4. Non-dimensional pressure gradients in the steel and the acrylic pipes at mixture velocity 2.6 m/s.

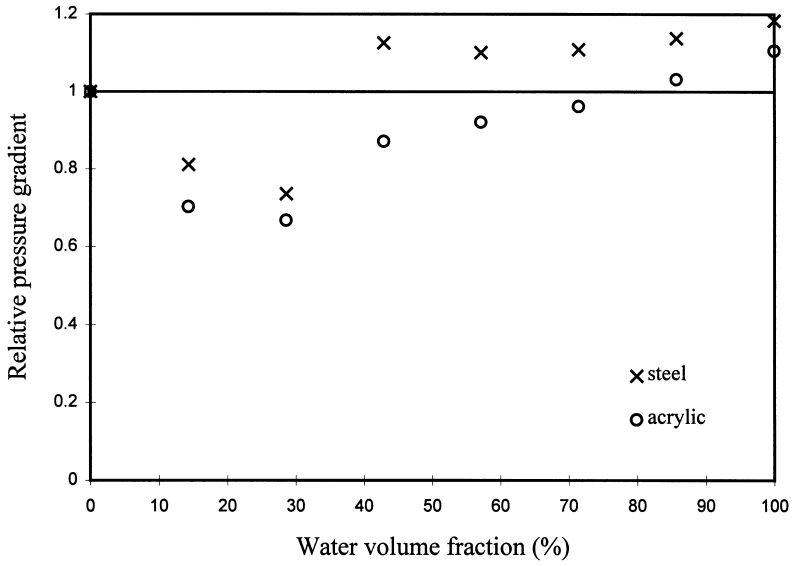

Fig. 5. Non-dimensional pressure gradients in the steel and the acrylic pipes at mixture velocity 3.0 m/s.

interface in the steel tube was more disturbed than in the acrylic tube. This would have led to higher pressure gradients in the steel pipe.

(2) At high mixture velocities (Figs. 4 and 5) the differences between the two tubes are less dramatic. At these mixture velocities the dispersed flow patterns prevail. Also both tubes show

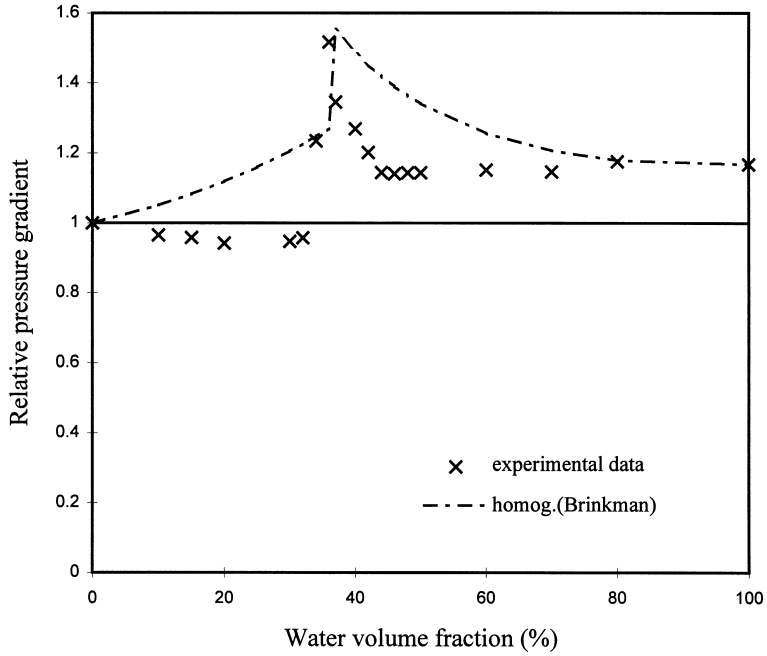

Fig. 6. Non-dimensional pressure gradient in the steel pipe at mixture velocity 2.1 m/s.

a drag reduction effect at low water volume fractions (oil continuous), while in the acrylic tube drag reduction can also be observed at high water volume fractions (water continuous) but to a lesser extent.

(3) At these high mixture velocities (Fig. 6) a sharp peak in pressure gradient, corresponding to phase inversion (see Section 4.3), appears. This peak though is observed at higher mixture velocities in the acrylic than in the steel tube, since the dispersed flow pattern is also established at higher mixture velocities in the acrylic than in the steel tube.

Apart from the differences in the flow patterns under the same flow conditions, the different wetting characteristics of the two tubes can also be responsible for these discrepancies in their pressure gradients. This would be true in particular at the high flow velocities where the same flow pattern (dispersed) is established in both pipes. Although the pipes were not prewetted by one of the phases before the experiments, it can be said that when water is the continuous phase the pipe is water wetted while when oil is the continuous phase the pipe is oil wetted, especially because each experiment was run for some time. Therefore when water is the continuous phase the contact angles of oil drops in water, in water wetted material, can be used, while when oil is the continuous phase the contact angles of water drops in oil, in oil wetted material, can be used. It can be seen from Table 4 that in oil continuous flows between the two pipes the difference in contact angles of the water drops is small (121.6 and 128.7 for the acrylic and the steel, respectively). On the other hand in water continuous flows, the difference in the contact angles of the oil drops is large (87.6 and 143.3 for the acrylic and the steel, respectively). The differences in pressure gradients in the two pipes are also smaller in oil continuous than in water continuous flows (Figs. 4 and 5).

4.3. Peak in pressure gradient

Phase inversion from oil continuous to water continuous dispersed flow occurred at around 37–40% input water volume fraction for both tubes. The peak in pressure gradient accompanying phase inversion was observed in the present data as is illustrated in Fig. 6, where the resulting relative pressure gradients for increasing water fraction at a mixture velocity of 2.1 m/s and for the stainless steel tube are shown. Also shown in this figure are the predictions of the homogeneous model with viscosity calculated from the Brinkman model (Eq. (12)). The general trend is predicted, as well as the total increase in the pressure gradient during phase inversion, but the model tends to overpredict the pressure gradient in the regions away from the peak.

4.4. Drag reduction

The above pressure gradient data during dispersed flows could be compared with the results reported by Pal (1993), who observed a drag reduction phenomenon during the pipe flow of oil–water dispersions. According to him, friction factors in turbulent dispersed flows were less than those expected when the measured laminar viscosity for the oil–water mixture and the standard single phase flow equations were used. In the present work the experimental friction factors during dispersed flow were plotted against the mixture velocity in Figs. 7–8 for oil and

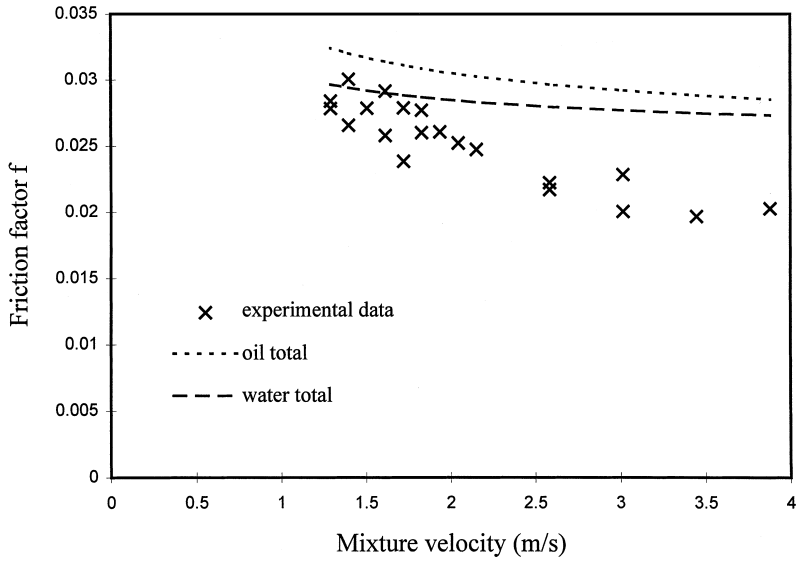

Fig. 7. Friction factor against mixture velocity in the steel pipe for oil continuous flows.

water continuous flows in the steel pipe. The data is compared with the friction factors for single phase flow of oil and water, at the same velocities as the two phase mixture.

The friction factors are significantly below the ones expected from the single phase data when oil is the continuous phase and about the same when water is the continuous phase. These results are similar to those observed by Pal (1993) who also found that the drag reduction phenomenon was higher in the oil continuous flows.

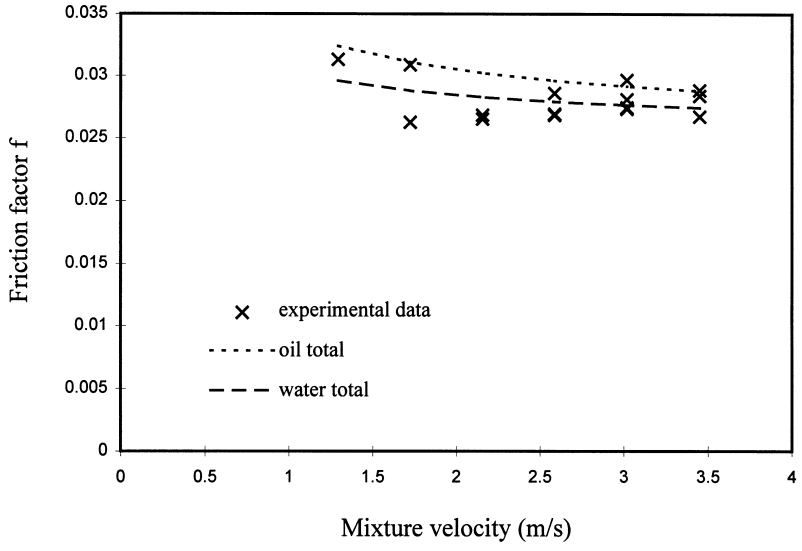

Fig. 8. Friction factor against mixture velocity in the steel pipe for water continuous flows.

Pal (1993) associated the drag reduction phenomenon in dispersed flows with the turbulence modification of the continuous liquid flow field due to the dynamic break-up/coalescence of the dispersed phase drops. Serizawa and Kataoka (1992) showed that the dispersed phase drops and the turbulent eddies of the continuous phase can interact in many different ways that depend on their relative sizes, these interactions affecting not only the drops but also the eddies. Owen (1986) had also observed a turbulence damping in the gas core of annular gas–liquid flow, which he attributed to the presence of liquid drops entrained from the liquid annular film. He based his explanation on the experimental values of the von Karman factor k, that had been calculated by other researchers from velocity profile measurements in the gas core. Turbulence damping occurred when these k values were lower than 0.4, which is the experimental value for turbulent single phase flows.

Although no velocity profile measurements were performed in the present work, the von Karman factor k can be calculated from the relationship that connects the single phase friction factor f with the Reynolds number and the pipe roughness. One such relationship, derived from dimensional analysis and the logarithmic velocity profile in turbulent pipe flow, is the following (Richardson, 1989):

$$\sqrt{\frac{8}{f}} = \frac{1}{k}\left[\ln\left(\frac{\mathrm{Re}\sqrt{f/4}}{1.0 + 0.1(\varepsilon_r/D)\mathrm{Re}\sqrt{f}}\right) - 2.54\right] + 5.35 \tag{14}$$

where f is the friction factor, k is the von Karman factor, Re is the Reynolds number, ε_r is the wall roughness and D is the pipe diameter. Eq. (14) is suitable for smooth and rough pipes in the transitional region of turbulent flow and is similar to the Colebrook (1939) formula. By using the experimental friction factors, the von Karman factor k can be estimated from Eq. (14), using the homogeneous model Reynolds number with the Dukler et al. (1964) viscosity relationship (Eq. (11)). The results for the steel pipe are shown in Fig. 9. For water continuous flows k is close to the expected value of 0.4. However, for oil continuous flows the k values are significantly less, particularly at high mixture velocities. The modified k values could be used in modelling the turbulent flow field during dispersed flow, since k is related to the mixing length which is often used in turbulence models (Massey, 1994). Modified k values, calculated from velocity profile measurements could also be used to estimate friction factors (from Eq. (14) and consequently pressure gradients in liquid–liquid dispersed flows.

4.5. Comparison with models

4.5.1. Empirical correlations

The experimental pressure gradient results were compared with the model proposed by Theissing (1980) which was described in Section 2.1. All the experimental data in the steel and the acrylic pipes were plotted in terms of X and Φ in Figs. 10–11, respectively. In view of the findings in Section 4.2, the experimental data were divided into three areas, namely low mixture velocities, high mixture velocities with oil as the continuous phase and high mixture velocities with water as the continuous phase. Although it does not show the different trends in pressure gradient in these three areas, the Theissing correlation seems to predict the

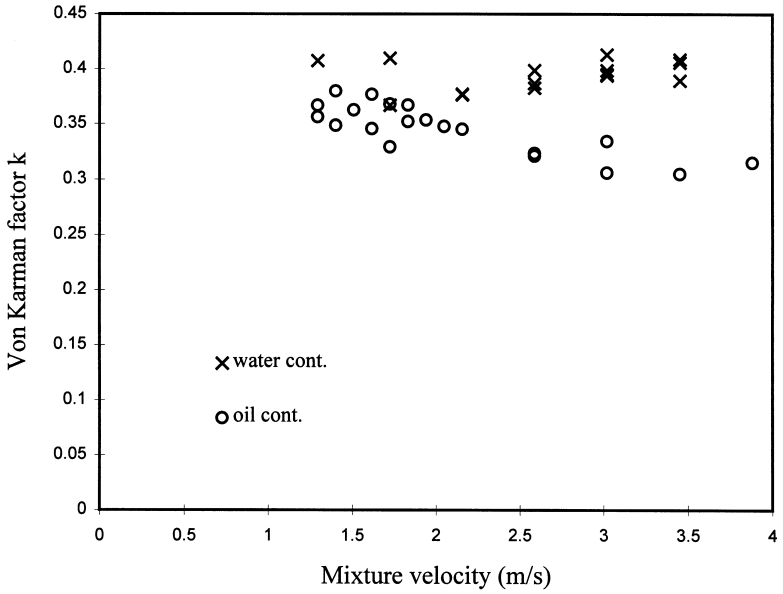

Fig. 9. k factor against mixture velocity in the steel pipe when the homogeneous model Reynolds number is used.

experimental data quite well. However, it should be remembered that plotting in terms of Φ implies the use of the square root of pressure gradient which improves the apparent accuracy.

4.5.2. Separated flow model

At low velocities the flow is stratified and it is relevant to use the separated flow model in which the phases flow in two layers separated by an interface across which momentum can be

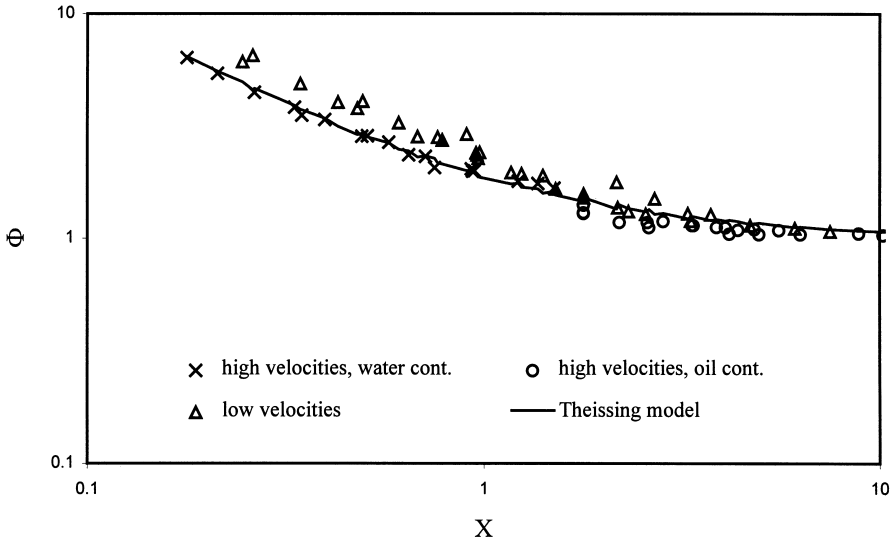

Fig. 10. Comparison of the experimental data with the Theissing model in the stainless steel pipe.

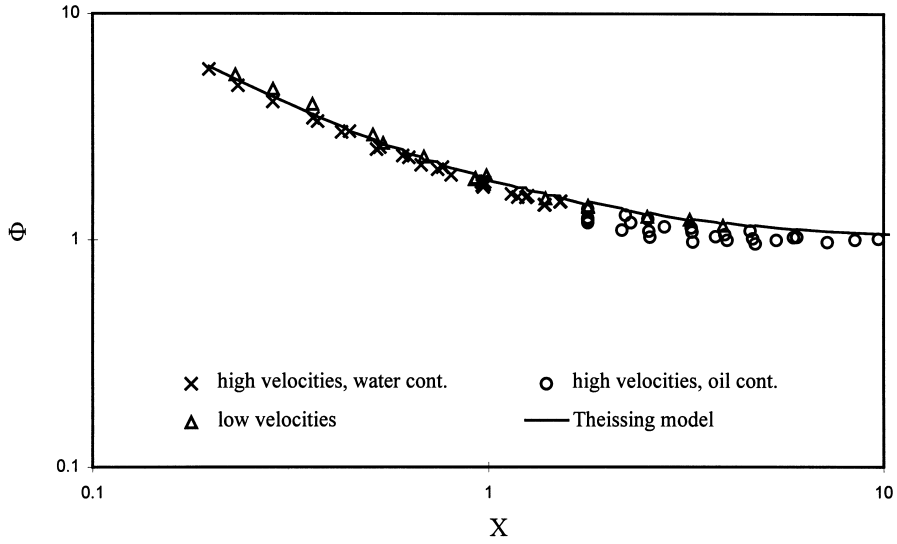

Fig. 11. Comparison of the experimental data with the Thiessing model in the acrylic pipe.

transferred (see Section 2.2.1). In applying the separated flow model, the wall friction factors for the oil and the water were estimated from the single phase flow values and the interfacial friction factor was assumed equal to the water-to-wall value.

The comparisons of the data with the separated flow model are shown in Figs. 12–13. The model underpredicts the data for the stainless steel tube and slightly overpredicts it for the acrylic tube. In the case of the steel tube the differences between the model and the experimental data can be explained in terms of increased interfacial mixing and consequently

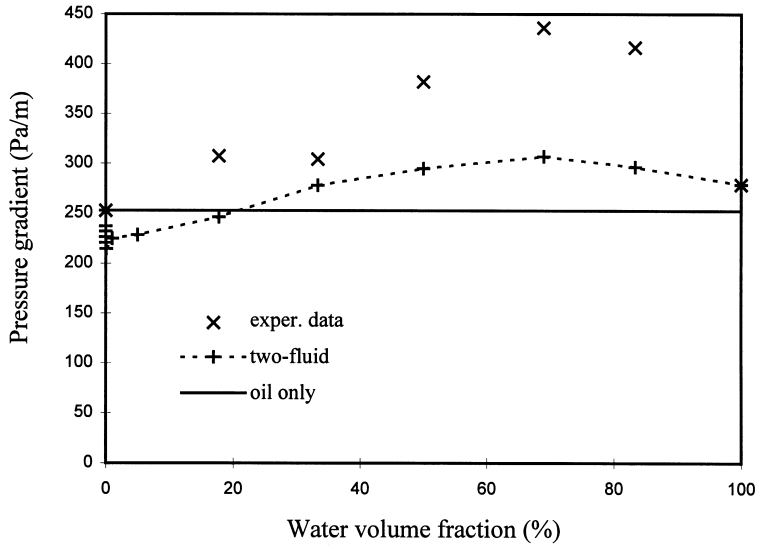

Fig. 12. Comparison of the pressure gradient data in the steel pipe with models, at 0.6 m/s mixture velocity.

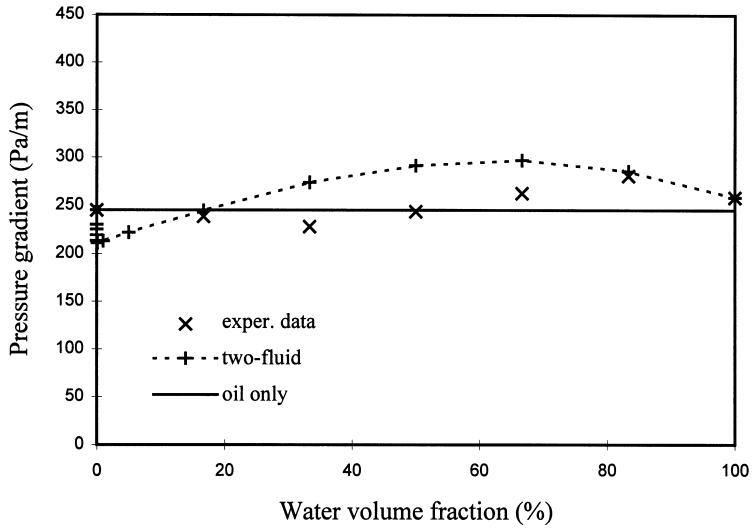

Fig. 13. Comparison of the pressure gradient data in the acrylic pipe with models, at 0.6 m/s mixture velocity.

increased interfacial friction factor. But at these velocities while the flow is still separated, drops of one phase into the other have appeared. Considering the changes in contact angles of the dispersed drops with the tube wall depending on the type of the dispersion and the tube material, as well as the appearance of drag reduction in the presence of drops in a continuous phase, there may be more than one phenomena which affect the resulting pressure gradient.

4.5.3. Homogeneous model

At high mixture velocities, the flow is dispersed and it is appropriate to compare the data with the homogeneous model using various definitions of the mixture viscosity (see Section 2.2.3). Comparisons of this type are shown in Figs. 14–15 where the mean viscosity has been calculated from the Dukler et al. expression (Eq. (11)) and from the Brinkman expression (Eq. (12)), respectively, using the input volume fractions of the two phases. The data for oil continuous flows is consistently overpredicted by both models whereas the data for water continuous flows is more closely approximated by the models. From Fig. 6 a peak in pressure gradient is expected at the phase inversion point but, apart from a step change, this peak is not shown in the widely spaced data in Figs. 14 and 15. The overprediction, especially in the oil continuous region, is due to the drag reduction phenomenon discussed in Section 4.4.

5. Conclusions

The following main conclusions were drawn from the work reported here:

• The material of the tube wall can strongly influence the pressure gradient during two-phase liquid–liquid flow. Pressure gradients under all conditions were higher in the steel than in the

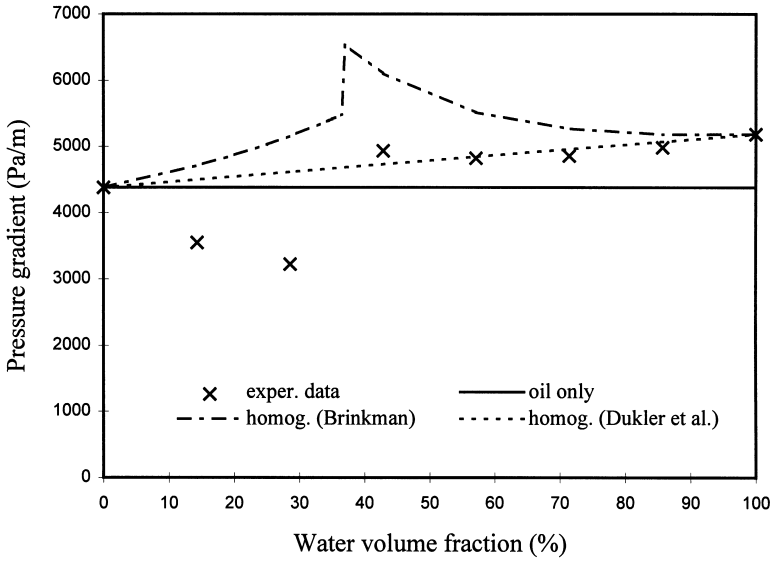

Fig. 14. Comparison of the pressure gradient data in the steel pipe with models, at 3.0 m/s mixture velocity.

acrylic tube for the same mixture velocities and flow volume fractions, the difference being greater than what would be expected from the difference in the wall roughness.

- For oil continuous flows significant drag reduction was observed in both pipes which was consistent with a reduction in the von Karman constant of up to about 35%.
- The data was compared with both empirical and phenomenological models. These models were in general in poor agreement with the data, probably as a result of wetting phenomena

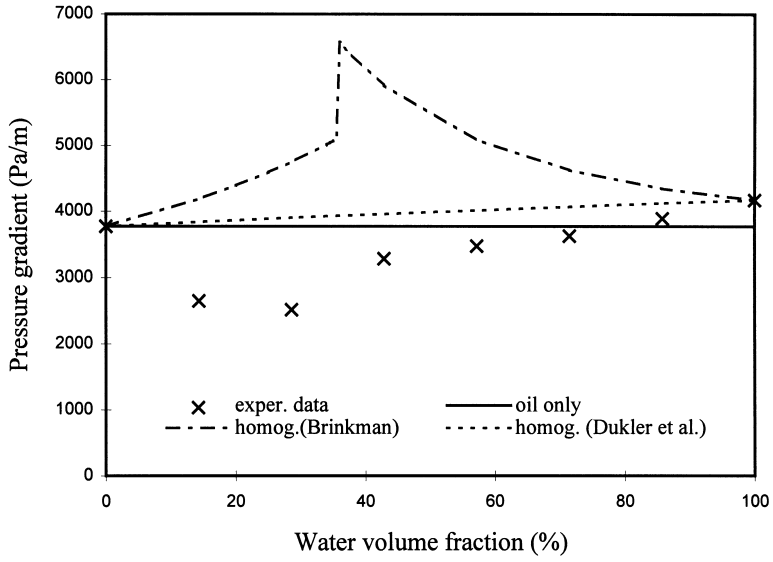

Fig. 15. Comparison of the pressure gradient data in the acrylic pipe with models, at 3.0 m/s mixture velocity.

and drag reduction effects mentioned above. Models need to be developed in the future which take into account these effects.

The variety and complexity of the phenomena that appear during two phase liquid–liquid flows are clearly a ripe field for further investigation. The differences between the two test sections used in the present work indicate the large role of the pipe material and especially its wetting properties, which are not usually taken into account. The role of drag reduction is also important and requires much further study.

Acknowledgements

The authors would like to express their gratitude to Norsk-Hydro for their contribution towards the construction of the experimental rig. P.A. is also grateful to Norsk-Hydro for providing financial support for the studentship. The authors would like to thank Dr. A. Kurban for contributing to the conduction of the experiments and S. Hardin for the results shown in Fig. 6.

References

Angeli, P., 1996. Liquid–liquid dispersed flows in horizontal pipes. Ph.D. Thesis, Imperial College, London.

Arirachakaran, S., Oglesby, K.D., Malinowsky, M.S., Shoham, O., Brill, J.P., 1989. An analysis of oil/water flow phenomena in horizontal pipes. SPE Paper 18836, SPE Prod. Operating Symp., Oklahoma, March 13–14, pp. 155–167.

Brauner, M., Moalem Maron, D., 1989. Two phase liquid–liquid stratified flow. Phys. Chem. Hydrodynamics 11, 487–506.

Brinkman, H.C., 1952. The viscosity of concentrated suspensions and solutions. J. Chem. Physics 20, 571.

Cengel, J.A., Faruqui, A.A., Finnigan, J.W., Wright, C.H., Knudsen, J.G., 1962. Laminar and turbulent flow of unstable liquid–liquid emulsions. AIChE J. 8, 335–339.

Charles, M.E., Govier, G.W., Hodgson, G.W., 1961. The horizontal pipeline flow of equal density oil–water mixture. Can. J. Chem. Eng. 39, 27–36.

Charles, M.E., Lilleleht, L.U., 1966. Correlation of pressure gradients for the stratified laminar-turbulent pipeline flow of two immiscible liquids. Can. J. Chem. Eng. 44, 47–49.

Charles, M.E., Redberger, P.J., 1962. The reduction of pressure gradients in oil pipelines by the addition of water: numerical analysis of stratified flow. Can. J. Chem. Eng. 40, 70–75.

Colebrook, C.F., 1939. Turbulent flow in pipes, with particular reference to the transition region between the smooth and rough pipe laws. J. Inst. Civ. Eng. 11, 133–156.

Dukler, A.E., Wicks, M., Cleveland, R.G., 1964. Pressure drop and hold-up in two-phase flow. AIChE J. 10, 38–51.

Efthimiadu, I., Kocianova, E., Moore, I.P.T., 1994. Behaviour of concentrated liquid–liquid dispersions in tube flow and in static mixers. In: Proc. The 1994 IChemE Research Event, vol. 2. pp. 1020–1022.

Faruqui, A.A., Knudsen, J.G., 1962. Velocity and temperature profiles of unstable liquid–liquid dispersions in vertical turbulent flow. Chem. Eng. Sci. 17, 897–907.

Guilinger, T.R., Grislingas, A.K., Erga, O., 1988. Phase inversion behaviour of water–kerosine dispersions. Ind. Eng. Chem. Res. 27, 978–982.

Guzhov, A., Grishin, A.D., Medredev, V.F., Medredeva, O.P., 1973. Emulsion formation during the flow of two liquids in a pipe. Neft Khoz 8, 58–61 (in Russian).

Hall, A.R.W., Hewitt, G.F., 1993. Application of two-fluid analysis to laminar stratified oil–water flows. Int. J. Multiphase Flow 19, 711.

Kurban, A.P.A., 1997. Stratified liquid–liquid flow. Ph.D. Thesis, Imperial College London.

Kurban, A.P.A., Angeli, P., Mendes-Tatsis, M.A., Hewitt, G.F., 1995. Stratified and dispersed oil–water flows in horizontal pipes. In: Proc. The 7th International Conference on Multiphase Production, Cannes, France. Mech. Eng. Publications, London, pp. 277–291.

Lockhart, R.W., Martinelli, R.C., 1949. Proposed correlation of data for isothermal two-phase, two-component flow in pipes. Chem. Eng. Prog. 45, 39–48.

Luhning, R.W., Sawistowski, H., 1971. Phase inversion in stirred liquid–liquid systems. In: Proc. Int. Solvent Extr. Conf., The Hague. Society of Chemical Industry, London, pp. 873–887.

Martinez, A.E., Arirachakaran, S., Shoham, O., Brill, J.P., 1988. Prediction of dispersion viscosity of oil/water mixture flow in horizontal pipes. In: 63rd Annual Technical Conf. and Exhibition of SPE, SPE Paper 18221. Houston, Oct. 2–5, pp. 427–438.

Massey, B.S., 1994. Mechanics of Fluids, 6th ed. Chapman and Hall, p. 148.

McClarey, M.J., Mansoori, G.A., 1978. Factors affecting the phase inversion of dispersed immiscible liquid–liquid mixtures. AIChE Symp. Series 74, 134–139.

Moalem Maron, D., Brauner, N., Rovinsky, J., 1995. Analytical prediction of the interface curvature and its effects on stratified two-phase flow characteristics. Two-Phase Flow Model. Exp., 163–170.

Nädler, M., Mewes, D., 1995. The effect of gas injection on the flow of two immiscible liquids in horizontal pipes. Chem. Eng. Technol. 18, 156–165.

Owen, D.G., 1986. An experimental and theoretical analysis of equilibrium annular flows. Ph.D. Thesis, University of Birmingham, Birmingham, pp. 248–252.

Pal, R., 1993. Pipeline flow of unstable and surfactant-stabilised emulsions. AIChE J. 39, 1754–1764.

Richardson, S.M., 1989. Fluid Mechanics. Hemisphere Publishing Corporation, pp. 251–260.

Roscoe, R., 1952. The viscosity of suspensions of rigid spheres. Br. J. Appl. Phys. 3, 267–269.

Russell, T.W.F., Charles, M.E., 1959. The effect of the less viscous liquid in the laminar flow of two immiscible liquids. Can. J. Chem. Eng. 37, 18–24.

Russell, T.W.F., Hodgson, G.W., Govier, G.W., 1959. Horizontal pipeline flow of mixtures of oil and water. Can. J. Chem. Eng. 37, 9–17.

Selker, A.H., Sleicher, C.A., Jr., 1965. Factors affecting which phase will disperse when immiscible liquids are stirred together. Can. J. Chem. Eng. 43, 298–301.

Serizawa, A. and Kataoka, I., 1992. Dispersed flow-I. Paper presented at the 3rd Int. Workshop on Two-Phase Flow Fundamentals. Imperial College, London.

Stapelberg, H.H., Mewes, D., 1994. The pressure loss and slug frequency of liquid–liquid–gas slug flow in horizontal pipes. Int. J. Multiphase Flow 20, 285–303.

Taitel, Y., Dukler, A.E., 1976a. A model for predicting flow regime transitions in horizontal and near horizontal gas–liquid flow. AIChE J. 22, 47–55.

Taitel, Y., Dukler, A.E., 1976b. A theoretical approach to the Lockhart–Martinelli correlation for stratified flow. Int. J. Multiphase Flow 2, 591–595.

Theissing, P., 1980. A generally valid method for calculating frictional pressure drop in multiphase flow. Chem. Ing. Techn. 52, 344–345 (in German).

Valle, A., 1995. Private communication. Norsk Hydro A.S.

Ward, J.P., Knudsen, J.G., 1967. Turbulent flow of unstable liquid–liquid dispersions: drop sizes and velocity distributions. AIChE J. 13, 356–365.

Zigrang, D.J., Sylvester, N.D., 1985. A review of explicit friction factor equations. J. Energy Res. Technol. 107, 280–283.